

Synthesis and Stable-Ion Studies of Regioisomeric Acetylnitropyrenes and Nitropyrenyl Carbinols and GIAO-DFT Study of Nitro Substituent Effects on α -Pyrenyl Carbocations

Kenneth K. Laali,^{*,[a]} Maria A. Arrica,^[a] Takao Okazaki,^[b] and Scott D. Bunge^[a]

Keywords: Substituent effects / Arenes / Fused-ring systems / Carbocations / Density functional calculations

Several regioisomeric acetylnitropyrenes were synthesized from isomeric acetylpyrenes by mild protic nitration. Nitration of 1-acetylpyrene gave the 3-, 6-, and 8-nitro derivatives (with 8-nitro as the major isomer), from which the corresponding carbinols [NO₂-Py-CH(OH)CH₃; Py = pyrene] were synthesized. Isomeric 4-acetylnitropyrenes and their corresponding carbinols were synthesized by starting from hexahydropyrene through nitration/aromatization/reduction or aromatization/nitration/reduction sequences. The molecular structures of 4-acetyl-3-nitropyrene and 1-(6-nitropyren-1-yl) ethanol were established by X-ray analysis. Tetrahydropyrene was the starting point for the synthesis of isomeric nitro-2-acetylpyrenes. Low-temperature protonation of 1-acetyl-8-nitropyrene, 4-acetyl-3-nitropyrene, and 2-acetyl-6-nitropyrene in FSO₃H/SO₂ClF or in FSO₃H/SbF₅ (1:1)/SO₂ClF resulted in the formation of onium dication (by C=O and NO₂

protonation). Charge delocalization (pyrenium ion character) in the carboxonium ions is strongly influenced by the position of the carboxonium group, with the 4-acetyl-3-nitropyrene dication being the most delocalized. Superacid protonation of 1-(3-nitropyren-4-yl)ethanol gave a persistent onium dication rather than an α -pyrenyl carbocation. With all other isolated nitropyrenyl carbinol isomers, low-temperature protonation (with FSO₃H/SO₂ClF) led to polymerization within 5 min standing at dry-ice-acetone temperature. For these cases, nitro substituent effects on the α -pyrenyl carbocations were gauged by DFT and GIAO-DFT studies. An interesting relationship between the computed nitro tilt angles and the GIAO-derived charge delocalization modes was observed.

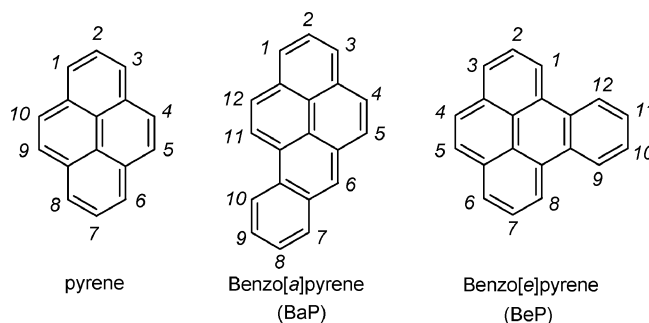
(© Wiley-VCH Verlag GmbH & Co. KGaA, 69451 Weinheim, Germany, 2008)

Introduction

Due to their mutagenic and carcinogenic activity and widespread presence in the environment, nitro derivatives of polycyclic aromatic hydrocarbons (nitroPAHs) have been the subject of intense synthesis and metabolism studies.^[1–5]

Among various classes of nitroPAHs that possess mutagenic and carcinogenic activity, isomeric nitrobenzo[*a*]pyrene (nitroBaP) and dinitroBaP (see structures for the parent PAHs and numbering systems) have been more extensively examined.^[6] It has been shown that nitro reduction and diol epoxide (DE) formation are both important in the metabolism of 1-nitro- and 3-nitroBaP.^[1,7] It was also demonstrated that the orientation of the nitro group is a determining factor in the observed mutagenicity.^[1,8] Whereas nitroPAHs possessing buttressed nitro group(s) are typically inactive or mildly active, planar nitroPAHs are sig-

nificantly more active. The hydroxylated and acetoxyated derivatives of nitroBaP and nitrobenzo[*e*]pyrene (nitroBeP) have received limited attention.^[9]



Focusing on mononitropyrene (NP) isomers, the mutagenicity order 4-NP > 2-NP > 1-NP was established, and nitro reduction and ring oxidation were both found to be important.^[10]

The involvement of the diol epoxide (DE) activation path in the metabolism of nitroBaP and other nitroPAHs focuses attention on nitro-substituted benzylic carbocations and the nitro substituent effect on their relative stability/reactivity.

By using protonation as a model reaction for the generation of electrophiles under stable-ion conditions,^[11] in several earlier studies we reported on nitro group diproton-

[a] Department of Chemistry, Kent State University, Kent, OH 44242, USA
Fax: +1-330-672-3816
E-mail: kllaali@kent.edu

[b] Department of Chemistry for Materials, Mie University, Tsu 514-8507, Japan

Supporting information for this article is available on the WWW under <http://www.eurjoc.org/> or from the author.

ation in sterically crowded nitropyrenes, and the formation of dihydroxyiminium-(oxoiminium) pyrenium dications, and on nitro group cyclization to generate persistent oxazoline (and 1,2-oxazine) pyrenium ions.^[12,13]

In other studies from this laboratory, a series of regioisomeric α -pyrene-substituted carbinols were synthesized, from which the corresponding isomeric α -pyrenyl carbocations were generated as models for the bay-region carbocations formed by the diol epoxide (or epoxide) of BaP and BeP.^[11,14,15] This study established the relative stability order shown in Figure 1.

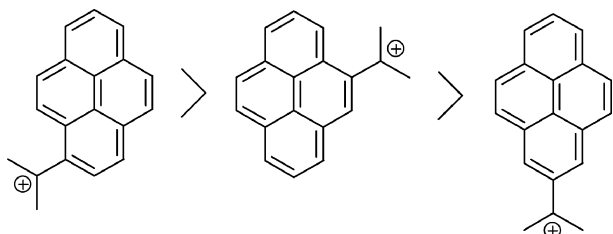


Figure 1. Relative stability order in regioisomeric α -pyrenyl carbocations.

In a separate study,^[16] persistent carboxonium-pyrenium dications were generated in $\text{FSO}_3\text{H}/\text{SbF}_5(4:1)/\text{SO}_2\text{ClF}$ from regioisomeric monoacetyl and monobenzoyl-substituted pyrenes, whereas with diacetyl- and dibenzoylpyrenes dicarboxonium ions were formed. It was found that the carboxonium group could strongly modulate charge delocalization into the pyrene moiety as a function of substitution position, and it proved to be a robust electron-withdrawing substituent, whose electronic response is sensitive to steric factors.^[16]

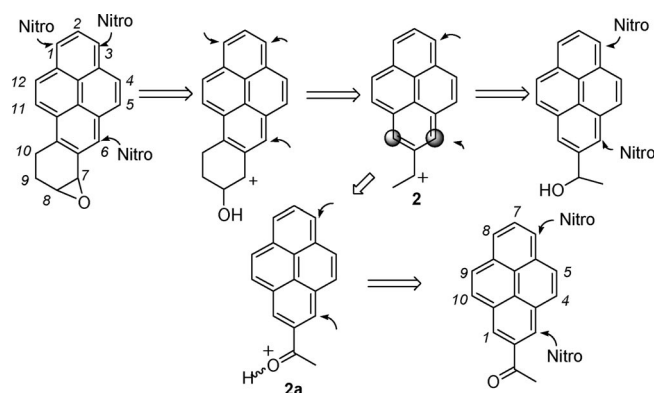
Earlier synthetic and metabolic studies demonstrated that the metabolism of nitroPAHs is rather complex, and depending on their structures, one or more of the following pathways could contribute: ring oxidation, ring oxidation/nitro reduction, nitro reduction, nitro reduction/esterification.^[1,7] Focusing on the isomeric nitroBaP, the metabo-

lism of 1-nitro and 3-nitro compounds were shown to involve bay-region oxidation, whereas for 6-nitroBaP, the 1,2-epoxide was suggested to be an intermediate.^[1]

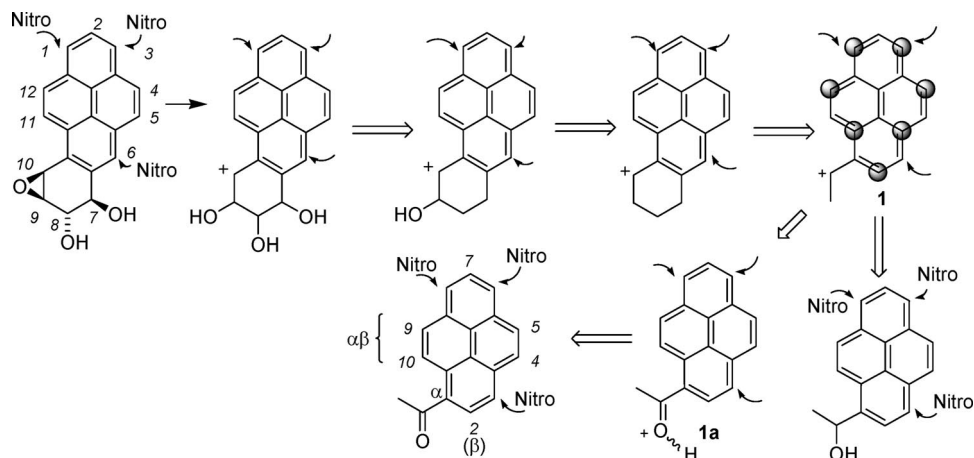
Given the proposed involvement of bay-region oxidation in the metabolism of nitroPAHs, the ultimate goal of the present investigation was to gauge nitro substituent effects on the regioisomeric α -pyrenyl carbocations directly by NMR spectroscopy (see Figure 1).

As highlighted in Schemes 1 and 2, our model study considered carbocations **1** and **2** to represent simplified models for the 9,10-epoxide (bay region) and the 7,8-epoxide of isomeric nitroBaPs, respectively. The charge delocalization mode in carbocation **1**, as derived from earlier work,^[14,15] is highlighted in the schemes as dark circles. There is significant p- π overlap in carbocation **1**, and positive charge is extensively delocalized throughout the periphery at alternating sites as indicated.

By contrast, carbocation **2** exhibits limited p- π overlap and has a narrow delocalization path (Scheme 2). It is, therefore, significantly less stable (has higher energy) than **1**.



Scheme 2. Nitro substituent effects on model carbocation **2** derived from isomeric nitro carbinols, with carboxonium ions **2a** acting as surrogate for **2** (dark circles signify charge delocalization mode).



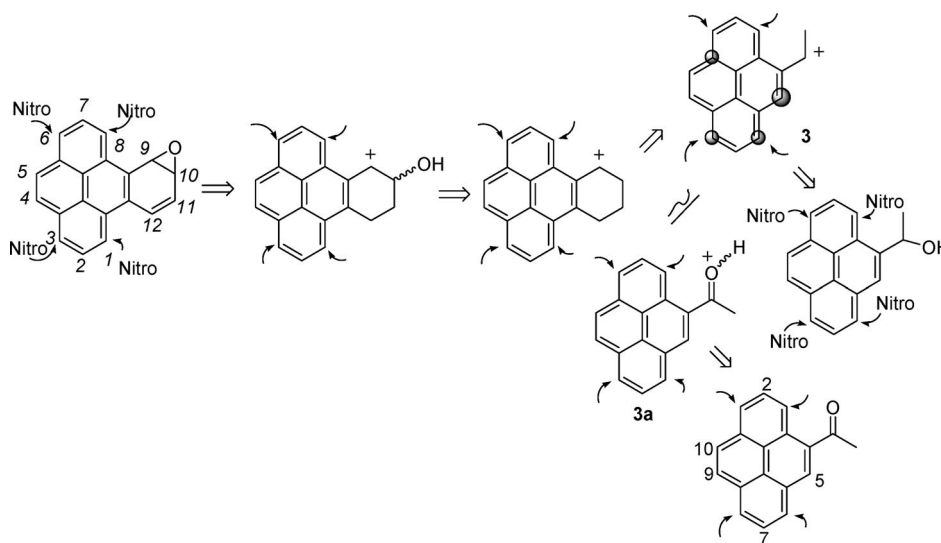
Scheme 1. Nitro substituent effects on model carbocation **1** derived from isomeric nitro carbinols, with carboxonium ions **1a** acting as surrogate for **1** (dark circles signify charge delocalization mode).

The regioisomeric carboxonium ions **1a** and **2a** (derived from isomeric nitroacetylpyrenes) are considered as surrogates for **1** and **2**. On the basis of these models, for carbocation type **1**, nitro substitution at C-6 and C-8 (corresponding to 3-nitroBaP and 1-nitroBaP) should have a more pronounced carbocation destabilization effect relative to that of 3-nitro (corresponding to 6-BaP), whereas for carbocation type **2**, nitro substitution at C-1/C-3 (corresponding to 6-nitroBaP) should be more strongly destabilizing.

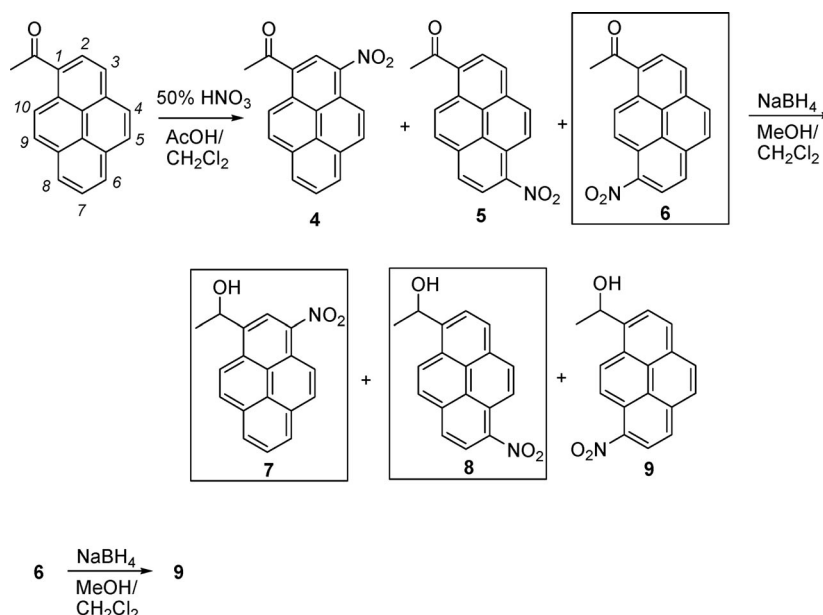
Similar considerations could be applied to BeP and its bay-region epoxide^[17] in order to gauge nitro substitution

effects, as depicted in Scheme 3. Considering the previously established charge delocalization mode in carbocation type **3**,^[14] nitro substitution at C-6/C-8 would be expected to destabilize the carbocation the most, whereas C-1/C-3 substitution should be comparatively less destabilizing. In this instance, carboxonium ion **3a** could be considered as surrogate for **3**.

The present study reports on the synthesis of specific acetylnitropyrene isomers and nitropyrenyl carbinols and their low-temperature protonation outcomes, and DFT and GIAO-DFT studies of the isomeric nitropyrenyl carbocations are also detailed.



Scheme 3. Nitro substitution effects on model carbocations **3** by isomeric nitro carbinols, with carboxonium ions **3a** acting as surrogate for **3** (dark circles signify charge delocalization mode).



Scheme 4. Synthesis of isomeric nitro derivatives of 1-acetylpyrenes and isomeric nitropyrenyl carbinols.

Results and Discussion

Synthesis of Isomeric Nitro Derivatives of 1-Acetylpyrene and 1-Pyrenylethanol

Mild protic nitration of 1-acetylpyrene (Scheme 4) gave an isomeric mixture of C-3/C-6/C-8 mononitro derivatives (compounds **4**, **5**, and **6**) in a 1.3:1:2.9 ratio (from ^1H NMR spectroscopy). Separation of the three isomers by column chromatography proved to be challenging due to their similar polarities. Only 8-nitroacetyl derivative **6** was isolated in reasonable amounts from the crude isomeric mixture. In an effort to change the relative isomer ratios to enable the separation of the other isomers, nitration of 1-acetylpyrene was performed with other reagents. With NaNO_3 and NO_2BF_4 there were no appreciable changes in the relative proportions of the three nitro isomers, and with $\text{Cu}(\text{NO}_3)_2$ much of the starting material was recovered at the end of the reaction.

The corresponding carbinols (compound **7**, **8**, and **9**) were synthesized by reduction of the isomeric mixture of the nitro ketones by using NaBH_4 . Subsequent column chromatographic separation led to isolation of **7** (20%) and **8** (18%). Finally, carbinol **9** was directly synthesized by reduction of isolated **6** (62%). The molecular structure of **8** was determined by X-ray analysis (Figure 2 and Supporting Information). The C–N bond length is 1.461 Å, and the N–O bond lengths are 1.224 and 1.206 Å. The nitro group is only slightly tilted out of the aromatic plane ($\approx 14^\circ$).

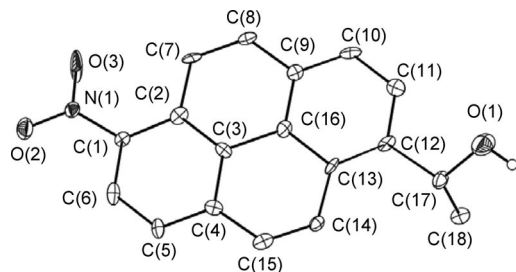


Figure 2. Thermal ellipsoid plot of nitro carbinol **8** (ellipsoids are drawn at 30% level).

Synthesis of the Nitro Derivatives of 4-Acetylpyrene and Their Corresponding Carbinols

1,2,3,6,7,8-Hexahydropyrene **10** was the starting point for the synthesis of the nitro derivatives of 4-acetylpyrene (Scheme 5). Acetylation of **10** gave the corresponding 4-acetyl derivative **11** in quantitative yield. At this stage, two different synthetic routes were considered in order to prepare the isomeric nitro derivatives. Path A (aromatization followed by nitration) gave a mixture of four nitro ketones (**12**, **12a**, **12b**, and **12c**; by using either nitric acid or NaNO_3 ; see Table 1). Of these four ketones, 4-acetyl-3-nitropyrene **12** was obtained in 34% yield, whereas all other fractions obtained by chromatography proved to be mixtures of two regioisomers.

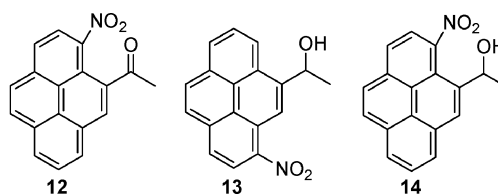
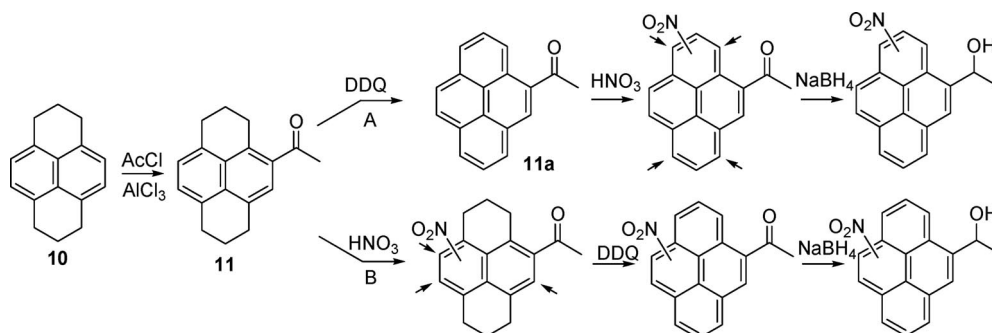


Table 1. Nitro isomer distribution (by NMR spectroscopy) by using different nitration conditions.

Isomer Ratios				
HNO_3	2.5 (34% yield)	0.9 ^[a]	1.3 ^[a]	1 ^[a]
NaNO_3	1	1 ^[b]	1.4 ^[b]	1 ^[b]

[a] Specified isomers may be interchanged in this group. [b] Specified isomers may be interchanged in this group.

The molecular structure of compound **12** was confirmed by X-ray analysis (Figure 3 and Supporting Information). The C–N bond length is 1.462 Å, and the N–O bond lengths are 1.235 and 1.242 Å. Due to increased *peri* strain, the nitro group in **12** is tilted out of the plane of the aromatic periphery by 40.3° . The acetyl group is also tilted (by circa 42°).



Scheme 5. Synthesis of isomeric nitro derivatives of 4-acetylpyrenes and isomeric nitropyrenyl carbinols.

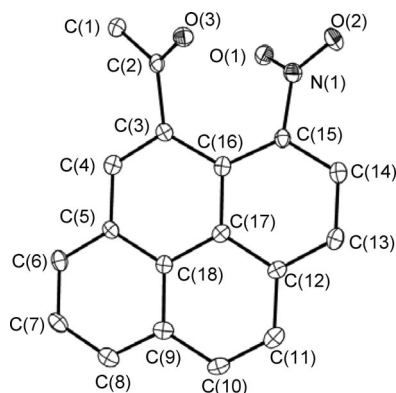


Figure 3. Thermal ellipsoid plot of **12** (ellipsoids are drawn at 30% level).

Direct reduction of the isomeric mixture of nitro ketones (also containing **12**) was then attempted by use of NaBH_4 . After 3 h, NMR spectroscopic analysis of the reaction mixture showed that compound **12** had not been reduced, whereas the other isomers had already been converted into alcohols. In a separate run, when isolated **12** was allowed to react overnight with an excess amount of NaBH_4 , conversion to the corresponding carbinol **14** took place in 82% yield. Column chromatography on the isomeric mixture of alcohols led to isolation of 6-nitro carbinol **13** (23%) along with 3-nitro carbinol **14** (21%). The corresponding 1-nitro and 8-nitro carbinols were obtained together as one fraction in 1:0.8 ratio (by NMR spectroscopy).

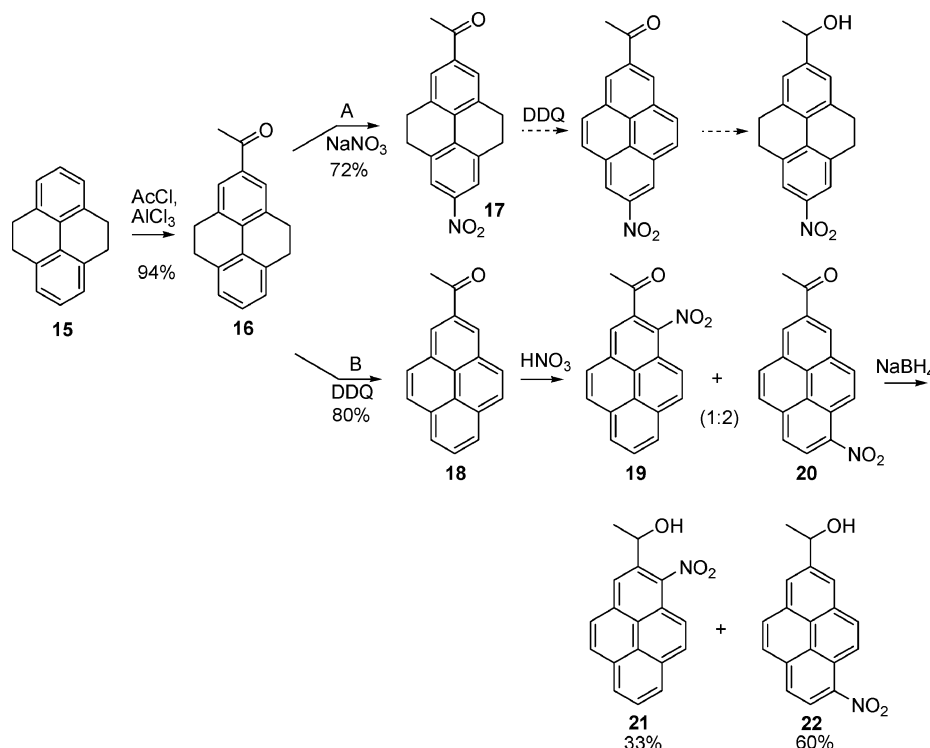
Although path B (nitration of **11**, followed by aromatization) could be executed efficiently, it turned out to be less rewarding, as numerous attempts to separate the isomeric nitro 4-acetyl derivatives proved unsuccessful. Direct reduction of the isomeric mixture, similarly yielded a mixture of isomeric carbinols that proved impossible to separate.

Synthesis of the Nitro Derivatives of 2-Acetylpyrene and Their Corresponding Carbinols

4,5,9,10-Tetrahydropyrene **15** served as the starting point for the synthesis of the nitro derivatives of 2-acetylpyrene (Scheme 6). Following path A, nitration proceeded efficiently (\rightarrow **17**), but subsequent aromatization proved unsuccessful by use of DDQ (2,3-dichloro-5,6-dicyano-1,4-benzoquinone), thus preventing the synthesis of the desired 7-nitro carbinol. By contrast, 2-acetylpyrene **18** was synthesized from **16** with DDQ in high yield (path B) and subsequent nitration by use of HNO_3 gave the 1-nitro and 6-nitro isomers **19** and **20** in 1:2 ratio, from which **20** could be isolated by chromatography. Reduction of the **19/20** isomeric mixture furnished the corresponding alcohols (**21/22**) and these were successfully separated by column chromatography.

Collective Outcome of the Synthetic Effort as a Basis for Stable-Ion Study

Focusing on the earlier discussed nitro substituent effects on relative carbocation stabilities and the model studies



Scheme 6. Synthesis of isomeric nitro derivatives of 2-acetylnitropyrenes and isomeric nitropyrenyl carbinols.

outlined in Schemes 1–3, the collective outcome of the synthetic effort is sketched in Figure 4, showing (by circles) the various nitro derivatives of isomeric acetylpyrenes and their corresponding carbinols that were isolated from different isomeric mixtures. These compounds constituted the starting points for the stable-ion study discussed below.

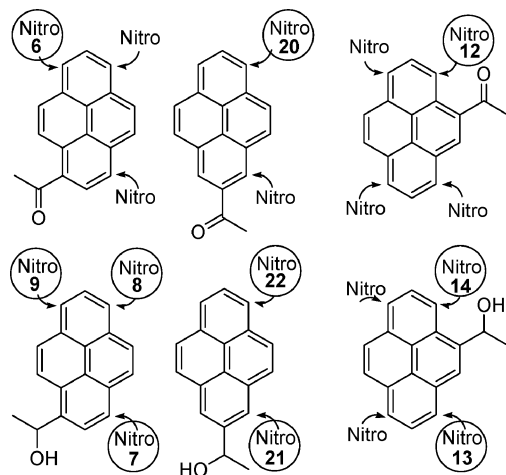


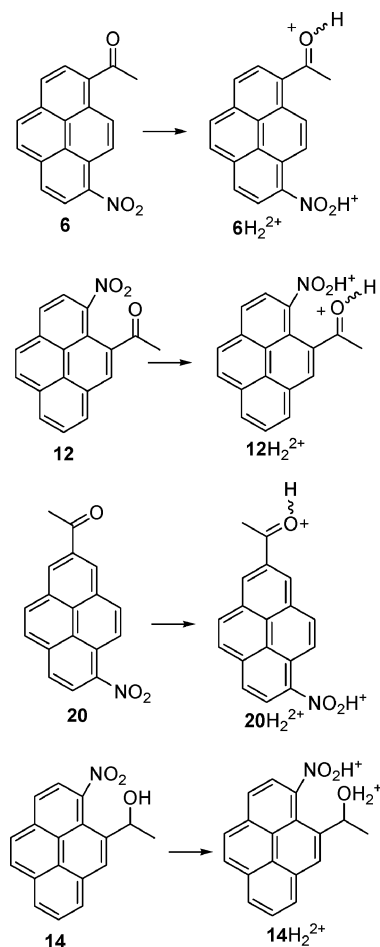
Figure 4. Sketch of the collective synthetic output (nitro isomers that were isolated are circled).

Stable-Ion Study

Low-temperature protonation (at dry-ice-acetone temperature) of 1-acetyl-8-nitropyrene **6**, 4-acetyl-3-nitropyrene **12**, and 2-acetyl-6-nitropyrene **20** (as highlighted in Figure 4) with $\text{FSO}_3\text{H}/\text{SO}_2\text{ClF}$ or $\text{FSO}_3\text{H}/\text{SbF}_5$ (1:1)/ SO_2ClF resulted in the formation of nitro-protonated carboxonium ions 6H_2^{2+} , 12H_2^{2+} , and 20H_2^{2+} (Scheme 7). The ^1H and ^{13}C NMR spectroscopic data for the dications are gathered in Schemes S1 and S2, respectively (see Supporting Information).

We showed previously that isomeric acetyl- and benzo-ylpyrenes form carboxonium–pyrenium dications in these media.^[16] The comparison underscores the impact of the $-\text{NO}_2\text{H}^+$ group as a highly powerful electron-withdrawing substituent. The conformation of the carboxonium group was established in each case through NOE difference spectra. Whereas carboxonium ions 6H_2^{2+} and 20H_2^{2+} exhibit limited charge delocalization on the basis of $\Delta\delta(^{13}\text{C})$ values, 12H_2^{2+} shows extensive p– π overlap between CO^+ and the pyrenyl π system. Interestingly, the ring carbon atom bearing the $-\text{NO}_2\text{H}^+$ group is bypassed to minimize destabilization of the system.

Focusing on the stable-ion study of the regioisomeric carbinols, low-temperature reaction (-60°C) of **14** with $\text{FSO}_3\text{H}/\text{SO}_2\text{ClF}$ gave a deep-blue solution whose NMR spectroscopic data (Schemes S1 and S2, Figure S3; Supporting Information) were most compatible with the formation of the corresponding onium dication 14H_2^{2+} (by OH and NO_2 protonation), ruling out an α -pyrenyl carbocation (see also further discussion on the computational aspects). Attempts to bring about dehydration by raising the tem-



Scheme 7. Low-temperature protonation of isomeric acetylnitropyrenes and nitropyrenyl carbinols.

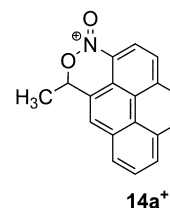
perature (up to -20°C) or by protonation with the stronger superacid $[\text{FSO}_3\text{H}/\text{SbF}_5$ (1:1)/ $\text{SO}_2\text{ClF}]$ gave the same result. The $-\text{CH}(\text{Me})\text{OH}_2^+$ signal of 14H_2^{2+} is deshielded by ≈ 22 ppm from that of **14**. Charge delocalization mode in 14H_2^{2+} and 12H_2^{2+} are rather similar, but the magnitude of the $\Delta\delta(^{13}\text{C})$ values are larger in 12H_2^{2+} . The isomeric nitro carbinols **13**, **21**, and **22** were similarly treated at low temperature with $\text{FSO}_3\text{H}/\text{SO}_2\text{ClF}$. However, in these cases, following rapid initial protonation (formation of clear-colored solutions), polymerization set in within 5 min (formation of viscous solid materials in the NMR tubes). In order to gauge the nitro substituent effect in these systems we focused our efforts on computational studies.

Computational Studies

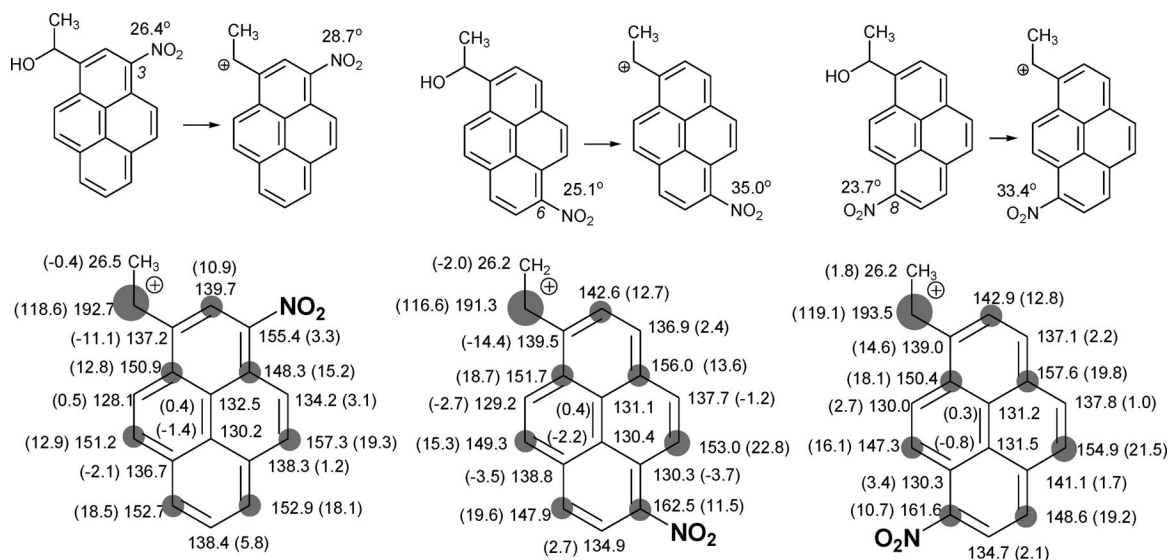
The isomeric nitropyrenyl carbinols and their derived carbocations (as sketched in Schemes 1–3) were computed by DFT method at the B3LYP/6-31G(d) level. Table S3 (Supporting Information) presents the energy data. The three isomeric nitro derivatives of carbocation **1** (3- NO_2 , 6- NO_2 , and 8- NO_2 ; see Scheme 1) were computed to have nearly identical energies (ΔG carbinol \rightarrow carbocation). For the two isomeric nitro carbocations derived from **2**, the 6-

nitro isomer is slightly more stable (by 1.4 kcal mol⁻¹) than the 1-nitro isomer. As for the isomeric nitro derivatives of carbocation **3**, structure optimization of the 3-nitro derivative resulted in nitro cyclization to form **14a⁺**. Among the remaining three nitro isomers, the 8-nitro derivative is less favored (by circa 3 kcal mol⁻¹), with the 1-nitro and 6-nitro derivatives having rather similar energies.

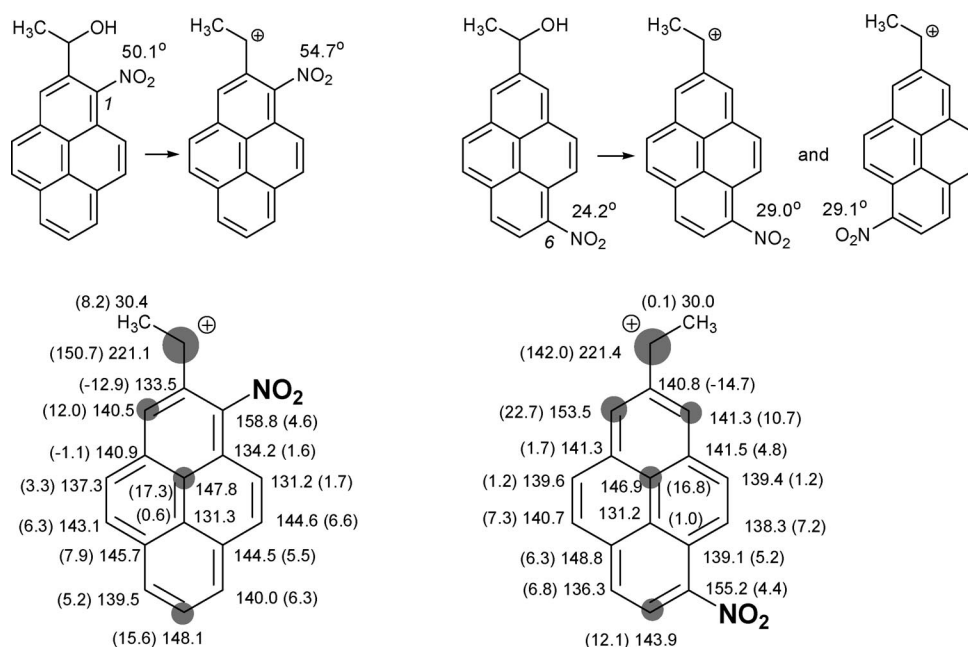
The NMR spectroscopic data for the carbocations and their carbinol precursors were computed by the GIAO-DFT method at the B3LYP/6-311+G(d,p)//B3LYP/6-31G(d) level, from which the charge delocalization modes



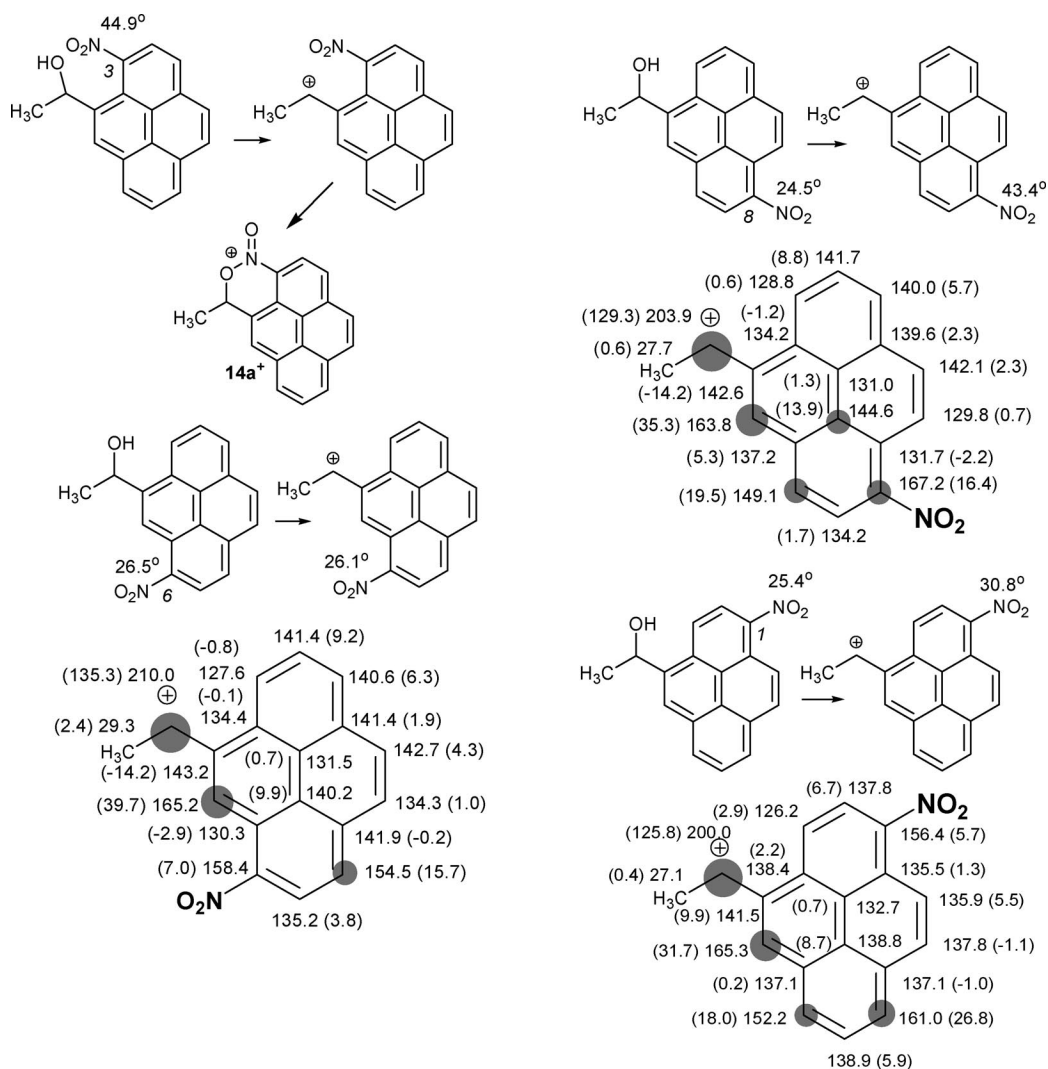
were derived for various isomers on the basis of the magnitude of the $\Delta\delta(^{13}\text{C})$ values. The data are sketched in Schemes 8–10. Also included in these schemes are the computed nitro tilt angles for various carbinol/carbocation



Scheme 8. Relationship between nitro group tilt angle and the GIAO-derived charge delocalization modes in the isomeric carbocations of type 1 [$\Delta\delta(^{13}\text{C})$ values relative to carbinols in parenthesis; dark circles are roughly proportional to $\Delta\delta(^{13}\text{C})$; threshold was set to 10 ppm].



Scheme 9. Relationship between nitro group tilt angle and the GIAO-derived charge delocalization modes in the isomeric carbocations of type 2 [$\Delta\delta(^{13}\text{C})$ values relative to carbinols in parenthesis; dark circles are roughly proportional to $\Delta\delta(^{13}\text{C})$; threshold was set to 10 ppm].



Scheme 10. Relationship between nitro group tilt angle and the GIAO-derived charge delocalization modes in the isomeric carbocations of type 3 [$\Delta\delta(^{13}\text{C})$ values relative to carbinols in parenthesis; dark circles are roughly proportional to $\Delta\delta(^{13}\text{C})$: threshold was set to 10 ppm].

pairs. Most remarkable are the changes in the nitro tilt angles upon carbinol \rightarrow carbocation transformation.

By focusing on the nitro derivatives of carbocation **1** and by comparing the GIAO-derived charge maps with changes in the nitro tilt angles (Scheme 8), it can be seen that when the nitro group is placed in a position with limited positive charge localization (3-nitro), minimal changes occurs in the nitro tilt angle upon ionization. By contrast, nitro substitution at sites bearing significant positive charge results in a notable increase in the tilting of the nitro group as a way to minimize repulsive interactions and to lower the energy of the system. This process rationalizes the computed similar relative energies of the three isomers. The nitro tilting approach enables all three isomeric carbocations to achieve regular and extensive charge delocalization throughout the periphery. The computed chemical shift at the carbocation centers are in the 191–193 ppm range.

Changes in the nitro tilt angle in the carbocations of type **2** is minimal, as in both isomers the nitro group is substi-

tuted in sites bearing limited positive charge (Scheme 9).

Type **2** carbocations are minimally delocalized, and the computed chemical shift at the carbocation centers is ca. 221 ppm.

Focusing on carbocations of type **3** (Scheme 10), the *peri*-substituted 1-nitro carbocation cyclized upon structure optimization (\rightarrow **14a⁺**) (see ref.^[11–13] for other, experimentally observed, examples of nitro cyclization in pyrenium ions; see also further discussion). Changes in the nitro tilt angle upon ionization in the 6-nitro and 1-nitro isomers are minimal, whereas in the case of the 8-nitro isomer there is significant nitro tilting. These patterns fit in with the GIAO-derived charge maps, showing that only the 8-nitro group is at a site where positive charge accumulates. The magnitude of positive charge delocalization in type **3** carbocations is in between those of types **1** and **2** (as was the case with the unsubstituted regioisomeric carbocations), and the computed chemical shift for the carbocation center is in the 200–210 ppm range.

In order to bridge the model GIAO-DFT study with the experimentally observed onium dications, bearing in mind that in the superacid studies the nitro group will be protonated, structure optimizations were extended to nitro-protonated α -pyrenyl carbocations.

Relative energies for various isomeric dications are included in Table S3 (Supporting Information). Among the three isomeric nitro derivatives of dication type **1**, the 6- and 8-nitro isomers are equally favored, whereas the 3-nitro isomer is ≈ 3 kcal mol^{–1} less stable. Stability difference between the two isomeric type **2** dications (1-nitro vs. 6-nitro isomer) is much greater relative to the monocations, favoring the 6-nitro isomer by 11 kcal mol^{–1}. For the isomeric dications of type **3**, the stability order 1-NO₂ > 3-NO₂ > 6-NO₂ > 8-NO₂ is computed.

Scheme S4 (Supporting Information) presents a side-by-side comparison of the computed tilt angles in the isomeric dications with the GIAO-derived charge delocalization modes. For the dications of type **1** and type **3** the –NO₂H⁺ group remains coplanar with the aromatic periphery and the charge maps show that in every case the ring carbon atom bearing the –NO₂H⁺ group is bypassed to minimize charge repulsion. This is achieved through subtle changes in the charge delocalization modes, which in most cases create adjacent positive charges on 2–3 ring carbon atoms. The ring carbon atom bearing the –NO₂H⁺ group is in fact shielded relative to the nitro carbinol precursors. Only the *peri*-NO₂H⁺ group is tilted out of the aromatic plane due to steric compression; in this case no nitro cyclization is observed. The computed carbocation centers are in the 222–224 ppm range in type **1** dications and the 221–242 ppm range in type **3** dications.

For the type **2** dications, only the *ortho*-NO₂H⁺ group is forced out of the aromatic plane and charge delocalization maps show changes resulting in adjacent positive charge formation in the periphery and shielding of the ring carbon atom bearing the –NO₂H⁺ group. The computed carbocation centers in type **2** dications are in the 233–244 ppm range.

Returning to stable-ion study of carbinol **14**, although the experimental NMR spectroscopic data are fully compatible with the proposed formation of onium dication **14H₂²⁺**, they could not definitively exclude the formation of **14a⁺** (formed upon structure optimization starting from *peri*-substituted 1-nitro carbocation). In an effort to resolve the issue, GIAO-NMR spectroscopic data were computed for **14H₂²⁺** and **14a⁺**, and the charge delocalization maps were derived for comparison with the experimental data (Scheme S5, Supporting Information). This showed that limited charge delocalization occurs in **14a⁺**, and the overall charge delocalization pattern for **14H₂²⁺** is more compatible with the formation of an onium dication as suggested earlier.

Finally, it is worth pointing out that the charge delocalization maps derived on the basis of GIAO-NMR are in overall agreement with the patterns derived from changes in the computed NPA charges (Scheme S6, Supporting Information).

Summary and Conclusions

A series of isomeric acetylnitropyrenes and their regioisomeric carbinols were synthesized and in several cases individual isomers were isolated and characterized. These served as precursors to regioisomeric α -pyrenyl carbocations or carboxonium ions, considered as simplified models for epoxide ring opening in isomeric nitroBaP and nitroBeP.

Onium dications were generated from three isomeric nitroacetylnitropyrenes and from one nitro carbinol isomer under stable-ion conditions and their charge delocalization modes were determined on the basis of magnitude of experimental $\Delta\delta(^{13}\text{C})$ values. All other isomeric nitro carbinols polymerized on exposure to superacid. The structures, NMR chemical shifts, and charge delocalization modes in these systems were gauged by DFT and GIAO-DFT.

Nitro tilting was recognized as a mechanism by which α -pyrenyl carbocations can avoid charge–charge repulsion and thus lower their energies. Relative stability in the nitro derivatives of regioisomeric α -pyrenyl carbocations are in the order type **1** > type **3** > type **2**, which is the same as the relative stability order in the parent carbocations (as in Figure 1). By contrast, the protonated nitro group remains planar with the aromatic periphery and differences in charge delocalization mode occur, resulting in adjacent positive charge formation in the periphery and shielding of the carbon atom bearing the –NO₂H⁺ group.

Discovery of nitro tilting in the model carbocations observed in this study may be significant in the biochemistry of nitroBaP and nitroBeP compounds, for which metabolic studies underscored the involvement of the diol–epoxide activation path.

Experimental

General: ¹H, ¹³C, and 2D NMR spectra of the neutral substrates were recorded at 400 MHz with a Bruker Avance-400 instrument.

CDCl_3 was used as the solvent and as an internal reference ($\delta = 7.26/77.0$ ppm; coupling constants J in Hz). Low-temperature NMR spectroscopic studies were performed at 500 MHz with a Varian Inova-500 instrument at specified temperatures with CD_2Cl_2 serving as the internal lock and reference. Partial ^1H NMR assignments for several acetylnitropyrenes had been reported in the literature.^[18] The present study provides complete ^1H and ^{13}C NMR assignments for the isomeric acetylpyrenes, their nitro derivatives, and carbinol derivatives (see Scheme S4, Supporting Information, and the Experimental Section). Mass spectrometric analyses were performed with a Bruker Esquire-LC ESI ion-trap spectrometer system in the positive ion mode. The following instrumental settings were used: capillary: -4000 V; end-plate offset: -500 V; nebulizer (N_2): 7.0 psi; dry gas (N_2): 7.00 L min^{-1} ; dry temp: 250 °C; primary skimmer: 22.5 V; secondary skimmer: 4.0 V. The PAHs were analyzed as silver complexes by using AgOTf in MeOH .^[19] Molecular ion peaks for complexes with the ^{107}Ag isotope were used for the determination. IR spectra were recorded with a Bruker Vector 33 IR spectrometer as KBr pellets. CH_2Cl_2 and toluene were distilled from CaH_2 under an argon atmosphere prior the use. FSO_3H was freshly distilled twice in an all-glass apparatus under an atmosphere of dry nitrogen. SO_2ClF was available from previous studies in our laboratory.

General X-ray Crystal Structure Information: X-ray crystallography was performed by mounting a crystal onto a thin glass fiber from a pool of Fluorolube™ and immediately placing it under a liquid N_2 cooled N_2 stream with a Bruker AXS diffractometer. The radiation used was graphite monochromatized Mo-K_α radiation ($\lambda = 0.7107$ Å). The lattice parameters were optimized from a least-squares calculation on carefully centered reflections. Lattice determination, data collection, structure refinement, scaling, and data reduction were carried out by using the APEX2 (version 1.0–27) software package. Data collection parameters are given in Table S1 (Supporting Information). Each structure was solved by direct methods. This procedure yielded a number of the C, N, and O atoms. Subsequent Fourier synthesis yielded the remaining atom positions. The hydrogen atoms were fixed in positions of ideal geometry and refined within the X-SHELL software. These idealized hydrogen atoms had their isotropic temperature factors fixed at 1.2 or 1.5 times the equivalent isotropic U of the C atoms to which they were bonded. The final refinement of each compound included anisotropic thermal parameters on all non-hydrogen atoms. Compound **8** contained two structurally similar, but crystallographically nonequivalent, molecules per unit cell. Only one of the molecules is shown in Figure 2. In addition, the second molecule in **8** has an O atom that was found to be disordered over two positions (O4 and O4A). This disorder was modeled and the appropriate final formula was included in the final refinement. For additional information concerning data collection and final structural solutions of compounds **12** and **8** see the Supporting Information.

CCDC-695963 (for **12**) and -695964 (for **8**) contain the supplementary crystallographic data for this paper. These data can be obtained free of charge from The Cambridge Crystallographic Data Centre via www.ccdc.cam.ac.uk/data_request/cif.

General Procedure for the Synthesis of Acetylnitro Derivatives Starting from the Corresponding Acetylpyrenes: To a solution of the acetylpyrene derivative (100 mg, 0.4 mmol) in $\text{AcOH}/\text{CH}_2\text{Cl}_2$ (1:1, 5 mL) at room temperature was added 50% HNO_3 (0.04 mL). The reaction mixture was allowed to stir at room temperature, and the progress of the reaction was monitored by TLC. Once the starting material was totally consumed (usually 2–3 h), water was added, and the organic phase was extracted with CH_2Cl_2 (3×10 mL). The

combined organic extract was then washed with 10% NaOH and dried (MgSO_4). Evaporation of the solvent gave a mixture of isomers, which were separated by column chromatography.

1-Acetyl-8-nitropyrene (6): Partially recovered from the mixture of regioisomeric ketones as a bright-yellow solid after column chromatography on silica gel ($\text{EtOAc}/\text{hexane}$, 4:6). Yield: 16 mg (14%). ^1H NMR (400 MHz, CDCl_3 , r.t.): $\delta = 2.93$ (s, 3 H, Me), 8.15 (d, $J = 9.2$ Hz, 1 H, 4-H), 8.21 (d, $J = 8.8$ Hz, 2 H, 5-H and 6-H), 8.31 (d, $J = 8.4$ Hz, 1 H, 3-H), 8.46 (d, $J = 8.0$ Hz, 1 H, 2-H), 8.66 (d, $J = 8.4$ Hz, 1 H, 7-H), 8.91 (d, $J = 10$ Hz, 1 H, 10-H), 9.14 (d, $J = 10$ Hz, 1 H, 9-H) ppm. ^{13}C NMR (100 MHz, CDCl_3 , r.t.): $\delta = 30.6$ (CH_3), 123.0 (CH), 123.7 (CH), 123.9 (C), 124.1 (C), 124.6 (C), 125.4 (CH), 126.7 (CH), 127.7 (CH), 128.2 (C), 128.9 (2 CH), 130.4 (CH), 133.5 (C), 133.9 (C), 134.9 (C), 201.8 (CO) ppm. IR: $\tilde{\nu} = 1675, 1585, 1505, 1334, 1313, 1235, 1182, 864, 827$ cm^{-1} . MS (ES): $m/z = 685.1$ [$2\text{M} + \text{Ag}$] $^+$, 396.1 [$\text{M} + \text{Ag}$] $^+$, 350.0 [$(\text{M} - \text{NO}_2) + \text{Ag}$] $^+$.

2-Acetyl-6-nitropyrene (20): Obtained as a bright-yellow solid after column chromatography on silica gel (CH_2Cl_2). Yield: 55 mg (47%). ^1H NMR (400 MHz, CDCl_3 , r.t.): $\delta = 2.93$ (s, 3 H, Me), 8.13 (d, $J = 9.2$ Hz, 1 H, 5-H), 8.19 (d, $J = 8.4$ Hz, 1 H, 6-H), 8.29 (d, $J = 8.8$ Hz, 1 H, 4-H), 8.35 (d, $J = 9.6$ Hz, 1 H, 10-H), 8.69 (d, $J = 8.4$ Hz, 1 H, 7-H), 8.82 (d, $J = 1.2$ Hz, 1 H, 1-H), 8.84 (d, $J = 1.6$ Hz, 1 H, 3-H), 8.89 (d, $J = 9.6$ Hz, 1 H, 9-H) ppm. ^{13}C NMR (100 MHz, CDCl_3 , r.t.): $\delta = 27.1$ (CH_3), 122.7 (CH), 123.7 (CH), 124.6 (C), 124.8 (CH), 125.3 (C), 125.9 (C), 126.5 (CH), 126.8 (CH), 127.8 (CH), 130.1 (C), 130.9 (C), 131.2 (CH), 131.9 (CH), 135.2 (C), 135.6 (C), 143.3 (C), 198.0 (CO) ppm. IR: $\tilde{\nu} = 1686, 1630, 1557, 1505, 1334, 1309, 1212, 891, 841, 813, 706$ cm^{-1} . MS (ES): $m/z = 687.1$ [$2\text{M} + \text{Ag}$] $^+$, 398.0 [$\text{M} + \text{Ag}$] $^+$, 242.9 [$\text{M} - \text{NO}_2$] $^+$.

4-Acetyl-3-nitropyrene (12): Obtained as a red solid by nitration of 4-acetylpyrene after column chromatography on silica gel (CH_2Cl_2). Yield: 40 mg (34%). ^1H NMR (400 MHz, CDCl_3 , r.t.): $\delta = 2.93$ (s, 3 H, Me), 8.15 (d, $J = 8.8$ Hz, 1 H, 10-H), 8.17 (t, $J = 8.0$ Hz, 1 H, 7-H), 8.23 (d, $J = 9.2$ Hz, 1 H, 9-H), 8.26 (d, $J = 8.0$ Hz, 1 H, 1-H), 8.40 (dd, $J = 7.6$ and 2.8 Hz, 2 H, 6-H and 8-H), 8.52 (d, $J = 8.8$ Hz, 1 H, 2-H), 8.57 (s, 1 H, 5-H) ppm. ^{13}C NMR (100 MHz, CDCl_3 , r.t.): $\delta = 28.5$ (CH_3), 120.0 (C), 122.7 (CH), 124.3 (C), 125.5 (CH), 125.9 (C), 127.3 (CH), 127.6 (CH), 128.4 (CH), 128.8 (C), 129.3 (CH), 130.1 (CH), 130.9 (C), 131.2 (CH), 134.7 (C), 135.5 (C), 144.8 (C), 200.1 (CO) ppm. IR: $\tilde{\nu} = 1714, 1589, 1506, 1339, 1222, 1184, 1158, 856$ cm^{-1} . MS (ES): $m/z = 687.1$ [$2\text{M} + \text{Ag}$] $^+$, 396.0 [$\text{M} + \text{Ag}$] $^+$, 243.0 [$\text{M} - \text{NO}_2$] $^+$. For the X-ray data, see the Supporting Information.

2-Acetyl-7-nitro-4,5,9,10-tetrahydropyrene (17): To the solution of **16** (125 mg, 0.5 mmol) in acetic acid (20 mL; kept at 0 °C) was added a solution of NaNO_3 (42 mg, 0.5 mmol) in trifluoroacetic acid (10 mL). Acetic anhydride was then added, and the resulting solution was kept at 0 °C for 30 min and then for 3 h at room temperature. Water was then added, and the organic phase was extracted with CH_2Cl_2 (3×10 mL). The combined organic extract was washed with 10% NaOH and dried with MgSO_4 . Evaporation of the solvent gave a solid that was purified by column chromatography (CH_2Cl_2). Yield: 105 mg (72%). ^1H NMR (400 MHz, CDCl_3 , r.t.): $\delta = 2.92$ – 3.00 (m, 8 H), 3.00 (s, 3 H, CH_3), 7.72 (s, 2 H, 1-H and 3-H), 7.99 (s, 2 H, 6-H, 8-H) ppm.

General Procedure for Carbonyl Reduction: Under an argon atmosphere, the isomeric mixture resulting from nitration of a specific acetylpyrene (or a particular nitro isomer isolated following chromatographic separation; typically 0.35 mmol) was dissolved in $\text{MeOH}/\text{CH}_2\text{Cl}_2$ (1:1, 4 mL) and NaBH_4 (34 mg, 1 mmol) was

added in portions to the previous solution kept at 0 °C. The reaction mixture was allowed to stir at 0 °C for 15 min and then warmed up to room temperature. After 2–3 h, water was added, and the organic phase was extracted with CH₂Cl₂ (3 × 5 mL). The combined organic layer was washed with brine and dried (MgSO₄). The solvent was removed under vacuum to obtain a mixture of isomeric nitro alcohols, which were then purified by column chromatography.

1-(3-Nitropyren-1-yl)ethanol (7): Obtained as a yellow solid after column chromatography on silica gel (EtOAc/CH₂Cl₂, 1:9). Yield: 21 mg (20%). ¹H NMR (400 MHz, CDCl₃, r.t.): δ = 1.80 (d, *J* = 6.4 Hz, 3 H, CH₃), 2.23 (br. s, 1 H, OH), 5.99 (q, *J* = 6.4 Hz, 1 H, CHCH₃), 8.13 (t, *J* = 7.6 Hz, 1 H, 7-H), 8.29 (d, *J* = 9.6 Hz, 1 H, 9-H), 8.30 (d, *J* = 9.2 Hz, 1 H, 5-H), 8.32–8.35 (m, 2 H, 6-H and 8-H), 8.37 (d, *J* = 9.1 Hz, 1 H, 10-H), 8.83 (d, *J* = 9.2 Hz, 1 H, 4-H), 8.93 (s, 1 H, 2-H) ppm. ¹³C NMR (100 MHz, CDCl₃, r.t.): δ = 25.1 (CH₃), 66.9 (CH), 119.4 (CH), 121.6 (CH), 122.1 (CH), 123.9 (C), 124.1 (C), 125.5 (C), 127.1 (CH), 127.5 (CH), 127.7 (CH), 130.4 (C), 130.5 (C), 130.9 (CH), 131.1 (CH), 139.2 (C), 143.2 (C) ppm. IR: ν̄ = 3407 (br.), 1621, 1118, 964, 807, 668, 603 cm⁻¹. MS (ES): *m/z* = 691.2 [2M + Ag]⁺, 398.1 [M + Ag]⁺, 382.0 [(M – OH) + Ag]⁺, 336 [(M – OH – NO₂) + Ag]⁺, 274.0 [M – OH]⁺.

1-(6-Nitropyren-1-yl)ethanol (8): Obtained as a bright-yellow solid after repeated column chromatography on silica gel on the fraction that was enriched with this isomer. The percent recovery was 18% (18 mg). ¹H NMR (400 MHz, CDCl₃, r.t.): δ = 1.76 (d, *J* = 6.5 Hz, 3 H, Me), 2.42 (br. s, 1 H, OH), 5.95 (d, *J* = 6.5 Hz, 1 H, CHCH₃), 8.01 (d, *J* = 9.2 Hz, 1 H, 3-H), 8.04 (d, *J* = 8.4 Hz, 1 H, 8-H), 8.18 (d, *J* = 9.4 Hz, 1 H, 4-H), 8.26 (d, *J* = 8.0 Hz, 1 H, 9-H), 8.33 (d, *J* = 8.0 Hz, 1 H, 10-H), 8.44 (d, *J* = 9.2 Hz, 1 H, 2-H), 8.56 (d, *J* = 8.4 Hz, 1 H, 7-H), 8.74 (d, *J* = 9.4 Hz, 1 H, 5-H) ppm. ¹³C NMR (100 MHz, CDCl₃, r.t.): δ = 25.5 (CH₃), 67.3 (CH), 121.2 (CH), 122.6 (CH), 123.8 (CH), 124.0 (CH), 124.0 (C), 125.1 (C), 125.3 (C), 125.7 (CH), 126.8 (CH), 127.1 (C), 127.3 (CH), 129.4 (C), 131.5 (CH), 134.4 (C), 142.1 (C), 142.8 (C) ppm. IR: ν̄ = 3422 (br.), 1585, 1504, 1294, 1106, 844, 810, 710 cm⁻¹. MS (ES): *m/z* = 691.2 [2M + Ag]⁺, 398.0 [M + Ag]⁺, 382.0 [(M – OH) + Ag]⁺, 274 [M – OH]⁺. For X-ray data, see the Supporting Information.

1-(8-Nitropyren-1-yl)ethanol (9): Obtained by reduction of its corresponding nitro ketone isomer **6** (16 mg) as a yellow solid after column chromatography on silica gel (EtOAc/CH₂Cl₂, 1:9). Yield: 10 mg (62%). ¹H NMR (400 MHz, CDCl₃, r.t.): δ = 1.79 (d, *J* = 6.4 Hz, 3 H, Me), 2.15 (br. s, 1 H, OH), 6.03 (q, *J* = 6.4 Hz, 1 H, CHCH₃), 8.07 (d, *J* = 8.8 Hz, 1 H, 5-H), 8.16 (d, *J* = 8.4 Hz, 1 H, 6-H), 8.21 (d, *J* = 8.8 Hz, 1 H, 4-H), 8.34 (d, *J* = 8.0 Hz, 1 H, 3-H), 8.38 (d, *J* = 8.0 Hz, 1 H, 2-H), 8.62 (d, *J* = 10.0 Hz, 1 H, 10-H), 8.66 (d, *J* = 8.4 Hz, 1 H, 7-H), 8.93 (d, *J* = 9.6 Hz, 1 H, 9-H) ppm. ¹³C NMR (100 MHz, CDCl₃, r.t.): δ = 25.6 (CH₃), 67.4 (CH), 121.9 (CH), 122.7 (CH), 123.9 (CH), 123.9 (C), 124.4 (C), 124.5 (CH), 125.4 (C), 126.5 (C), 126.6 (CH), 126.7 (CH), 127.9 (CH), 130.5 (C), 130.9 (CH), 135.4 (C), 141.9 (C), 143.0 (C) ppm. IR: ν̄ = 3400 (br.), 2924, 1585, 1501, 1294, 1109, 851 cm⁻¹. MS (ES): *m/z* = 689.2 [2M + Ag]⁺, 399.1 [M + Ag]⁺, 382.0 [(M – OH) + Ag]⁺, 274 [M – OH]⁺.

1-(3-Nitropyren-4-yl)ethanol (14): Obtained by reduction of its corresponding nitro ketone isomer (42 mg) as a brown-yellow solid. Yield: 35 mg (82%). More of this compound was isolated out of the isomeric mixture of the carbinols, following column chromatography on silica gel (EtOAc/hexane, 4:6). Yield: 9 mg (21%). ¹H NMR (400 MHz, CDCl₃, r.t.): δ = 1.69 (d, *J* = 6.0 Hz, 3 H, Me), 2.21 (br. s, 1 H, OH), 5.50 (q, *J* = 6.0 Hz, 1 H, CHCH₃), 8.11 (d, *J* = 8.8 Hz, 1 H, 9-H), 8.13 (t, *J* = 7.6 Hz, 1 H, 7-H), 8.19 (d, *J* =

8.4 Hz, 1 H, 1-H), 8.22 (d, *J* = 8.8 Hz, 1 H, 10-H), 8.24 (d, *J* = 8.0 Hz, 1 H, 2-H), 8.32 (dd, *J* = 7.6 and 1.6 Hz, 1 H, 8-H), 8.34 (dd, *J* = 7.6 and 1.6 Hz, 1 H, 6-H), 8.66 (s, 1 H, 5-H) ppm. ¹³C NMR (100 MHz, CDCl₃, r.t.): δ = 25.3 (CH₃), 66.3 (CH), 121.3 (C), 122.1 (CH), 123.3 (C), 124.5 (CH), 126.1 (C), 127.1 (CH), 127.2 (2CH), 127.4 (CH), 129.1 (CH), 129.7 (CH), 130.3 (C), 130.8 (C), 134.2 (C), 138.6 (C), 145.4 (C) ppm. IR: ν̄ = 3494 (br.), 2969, 2924, 1585, 1508, 1336, 1103, 880, 846 cm⁻¹. MS (ES): *m/z* = 691.2 [2M + Ag]⁺, 400.1 [M + Ag]⁺, 274.0 [M – OH]⁺.

1-(6-Nitropyren-4-yl)ethanol (13): Obtained as a bright-yellow solid after column chromatography on silica gel (EtOAc/hexane, 4:6). Yield: 23 mg (23%). ¹H NMR (400 MHz, CDCl₃, r.t.): δ = 1.84 (d, *J* = 6.4 Hz, 3 H, Me), 2.30 (br. s, 1 H, OH), 5.88 (q, *J* = 6.8 Hz, 1 H, CHCH₃), 8.06 (d, *J* = 9.2 Hz, 1 H, 10-H), 8.11 (d, *J* = 8.4 Hz, 1 H, 8-H), 8.13 (t, *J* = 8.0 Hz, 1 H, 2-H), 8.21 (d, *J* = 8.8 Hz, 1 H, 9-H), 8.31 (d, *J* = 7.6 Hz, 1 H, 1-H), 8.59 (d, *J* = 7.2 Hz, 1 H, 3-H), 8.61 (d, *J* = 8.4 Hz, 1 H, 7-H), 9.05 (s, 1 H, 5-H) ppm. ¹³C NMR (100 MHz, CDCl₃, r.t.): δ = 24.6 (CH₃), 68.0 (CH), 117.5 (CH), 122.7 (CH), 123.2 (CH), 123.9 (C), 124.1 (CH), 124.3 (C), 124.4 (C), 126.7 (CH), 126.8 (CH), 127.7 (CH), 127.9 (C), 131.0 (CH), 131.4 (C), 134.7 (C), 143.1 (C), 144.9 (C) ppm. IR: ν̄ = 3407 (br.), 1621, 1509, 1117, 795, 688, 602 cm⁻¹. MS (ES): *m/z* = 689.1 [2M + Ag]⁺, 400.0 [M + Ag]⁺, 382.0 [(M – OH) + Ag]⁺, 336.0 [(M – OH – NO₂) + Ag]⁺, 273.0 [M – OH]⁺.

1-(1-Nitropyren-2-yl)ethanol (21): Obtained as a brown-yellow solid after column chromatography on silica gel (EtOAc/hexane, 6:4). Yield: 34 mg (33%). ¹H NMR (400 MHz, CDCl₃, r.t.): δ = 1.74 (d, *J* = 6.4 Hz, 3 H, Me), 2.49 (br. s, 1 H, OH), 5.40 (q, *J* = 7.2 Hz, 1 H, CHCH₃), 7.95 (d, *J* = 9.2 Hz, 1 H, 3-H), 8.06 (d, *J* = 8.8 Hz, 1 H, 10-H), 8.08 (t, *J* = 7.6 Hz, 1 H, 7-H), 8.15 (d, *J* = 8.8 Hz, 1 H, 10-H), 8.20 (d, *J* = 9.6 Hz, 1 H, 5-H), 8.23–8.27 (m, 2 H, 6-H and 8-H), 8.41 (s, 1 H, 1-H) ppm. ¹³C NMR (100 MHz, CDCl₃, r.t.): δ = 25.1 (CH₃), 66.3 (CH), 120.3 (CH), 122.1 (CH), 122.6 (C), 123.6 (C), 123.9 (C), 126.6 (CH), 126.9 (CH), 127.0 (CH), 127.0 (CH), 129.7 (CH), 130.3 (C), 130.7 (CH), 130.8 (C), 132.8 (C), 134.9 (C), 143.4 (C) ppm. IR: ν̄ = 3440 (br.), 2924, 1594, 1513, 1261, 1106, 799, 709 cm⁻¹. MS (ES): *m/z* = 691.1 [2M + Ag]⁺, 399.0 [M + Ag]⁺, 352.0 [(M – NO₂) + Ag]⁺, 274.1 [M – OH]⁺.

1-(6-Nitropyren-2-yl)ethanol (22): Obtained as a bright-yellow solid after column chromatography on silica gel (EtOAc/hexane, 6:4). Yield: 61 mg (60%). ¹H NMR (400 MHz, CDCl₃, r.t.): δ = 1.72 (d, *J* = 6.4 Hz, 3 H, Me), 2.45 (br. s, 1 H, OH), 5.37 (q, *J* = 6.4 Hz, 1 H, CHCH₃), 7.95 (d, *J* = 8.8 Hz, 1 H, 9-H), 8.01 (d, *J* = 8.4 Hz, 1 H, 8-H), 8.10 (d, *J* = 8.8 Hz, 1 H, 10-H), 8.13 (d, *J* = 9.6 Hz, 1 H, 4-H), 8.20 (d, *J* = 1.2 Hz, 1 H, 1-H), 8.24 (d, *J* = 1.2 Hz, 1 H, 3-H), 8.54 (d, *J* = 8.4 Hz, 1 H, 7-H), 8.72 (d, *J* = 9.6 Hz, 1 H, 5-H) ppm. ¹³C NMR (100 MHz, CDCl₃, r.t.): δ = 26.1 (CH₃), 70.4 (CH), 121.8 (CH), 122.5 (CH), 122.8 (C), 123.9 (CH), 124.1 (CH), 124.2 (C), 124.3 (C), 124.4 (CH), 126.9 (CH), 130.0 (C), 130.6 (CH), 130.9 (C), 131.3 (CH), 134.8 (C), 142.2 (C), 144.9 (C) ppm. IR: ν̄ = 3440 (br.), 2967, 1629, 1594, 1562, 1495, 1212, 949, 880, 862, 780, 705 cm⁻¹. MS (ES): *m/z* = 691.1 [2M + Ag]⁺, 399.0 [M + Ag]⁺, 382.0 [(M – OH) + Ag]⁺, 274.0 [M – OH]⁺.

General Procedure for Acetylation: Under an argon atmosphere to a suspension of AlCl₃ (73 mg, 0.55 mmol) in freshly distilled CH₂Cl₂ was slowly added acetyl chloride (43 mg, 0.55 mmol) at 0 °C. The reaction mixture was stirred at room temperature until a clear solution resulted. The temperature was once again lowered to 0 °C, and a solution of tetrahydropyrene or hexahydropyrene (0.5 mmol) dissolved in CH₂Cl₂ (2 mL) was then introduced into the previous solution. The reaction mixture was then allowed to stir for an additional 2 h at room temperature. HCl (10%) and

water were then added, and the two phases were separated. Following extraction with CH_2Cl_2 (3×10 mL), the combined organic extract was washed with brine and dried (MgSO_4). Evaporation of the solvent gave a yellow solid, which was used without further purification in the following steps.

4-Acetyl-1,2,3,6,7,8-hexahydropyrene (11): Yellow solid. Yield: 122 mg (98%). ^1H NMR (400 MHz, CDCl_3 , r.t.): δ = 1.98–2.11 (m, 4 H), 2.64 (s, 3 H, CH_3), 3.03–3.12 (m, 6 H), 3.28 (t, J = 6.0 Hz, 2 H), 7.17 (d, J = 7.0 Hz, 1 H), 7.21 (d, J = 7.0 Hz, 1 H), 7.38 (s, 1 H, 5-H) ppm.

2-Acetyl-4,5,9,10-tetrahydropyrene (16):^[20] Yellow solid. Yield: 116 mg (94%). ^1H NMR (400 MHz, CDCl_3 , r.t.): δ = 2.62 (s, 3 H, CH_3), 2.92 (m, 8 H, CH_2), 7.10 (d, J = 8.0 Hz, 2 H, 6-H and 8-H), 7.19 (t, J = 8.0 Hz, 1 H, 7-H), 7.68 (s, 2 H, 1-H and 3-H) ppm.

General Procedure for Aromatization: To a solution of the corresponding acetyltetrahydropyrene, acetylhexahydropyrene, or their nitro derivative (typically 0.4 mmol) was added DDQ (1.2 mmol) in dry toluene (40 mL), and the mixture was heated to reflux for 6 h. After cooling to room temperature, the reaction was stirred with a saturated sodium sulfite solution and filtered. The organic layer was separated after extraction with toluene, and the organic extract was washed with water (twice) and dried (MgSO_4). Evaporation of the solvent under reduced pressure gave the corresponding crude product, which was purified by column chromatography over silica gel.

4-Acetylpyrene (11a):^[16] Obtained as a brown solid after column chromatography (CH_2Cl_2). Yield: 76 mg (78%). ^1H NMR (400 MHz, CDCl_3 , r.t.): δ = 2.90 (s, 3 H, CH_3), 8.01–8.12 (m, 4 H), 8.22–8.29 (m, 3 H), 8.53 (s, 1 H, 5-H), 9.08 (dd, J = 8.0 and 0.8 Hz, 1 H, 3-H) ppm.

2-Acetylpyrene (18):^[16] Obtained as a brownish solid. Yield: 78 mg (80%). ^1H NMR (400 MHz, CDCl_3 , r.t.): δ = 2.88 (s, 3 H, CH_3), 8.02–8.23 (m, 7 H), 8.67 (s, 2 H, 1-H and 3-H) ppm.

Procedure for Stable-Ion Generation: The substrate (10–15 mg) was placed in a 5-mm NMR tube previously flushed with argon. Into the NMR tube, cooled to dry ice–acetone temperature was condensed SO_2ClF (1 mL). Then, FSO_3H (3–4 drops) or $\text{SbF}_5/\text{FSO}_3\text{H}$ (1:1, 2 drops) was added under argon, and the resulting solution was efficiently mixed (vortex). Finally, cold CD_2Cl_2 (3–4 drops) was introduced into the NMR tube, and the resulting solution was again mixed (vortex). The superacid solutions had the following colors: 6H_2^{2+} clear red; 12H_2^{2+} deep blue; 20H_2^{2+} deep purple; 14H_2^{2+} deep blue.

Quenching Experiments: The cold superacid solutions were poured into ice water–sodium hydrogen carbonate and extracted with CH_2Cl_2 . NMR spectroscopic analysis of the crude samples showed in all cases the recovery of the structurally intact nitro ketone derivatives.

Computational Protocols: Structures were optimized by using a C_1 molecular point group by the density function theory (DFT) method^[21] at B3LYP/6-31G(d) level^[22] with the use of the Gaussian 03 package.^[23] All computed geometries were verified by frequency calculations to have no imaginary frequencies. Energies are summarized in Table S3 (Supporting Information). Gibbs free energies were calculated at 25 °C. Natural population analysis (NPA) derived charges were computed at the same level.^[24] NMR chemical shifts were calculated by the GIAO^[25] method at the B3LYP/6-311+G(d,p)/B3LYP/6-31G(d) level. ^{13}C NMR chemical shifts were referenced to TMS (GIAO magnetic shielding tensor = 184.1 ppm in TMS; these values are related to the GIAO isotropic magnetic

susceptibility for ^{13}C), calculated with molecular symmetry of T_d at the same level of theory. The ring centers were defined as the simple average of Cartesian coordinates for all the carbon atoms in the ring. Planes of the rings were calculated by least-square methods by using coordinates of the all carbon atoms in the rings.

Supporting Information (see also the footnote on the first page of this article): Specific NMR assignments; X-ray analysis; GIAO NMR; charge delocalization maps and nitro tilt angles for the dications; GIAO-NMR and charge delocalization maps for 14H_2^{2+} and 14a^+ ; energy and Cartesian coordinates for the optimized structures by DFT calculations; charge delocalization maps based on NPA charges; selected NMR spectra.

Acknowledgments

We thank Prof. T. Yamato (Saga University, Japan) for kindly sending us a sample of tetrahydropyrene. Support of our work in the PAH area under “Reactive Intermediates of Carcinogenesis of PAHs” by the National Cancer Institute of the National Institutes of Health (2R15CA078235-02A1) is gratefully acknowledged.

- [1] P. P. Fu, M. W. Chou, F. A. Beland in *Polycyclic Aromatic Hydrocarbons Carcinogenesis: Structure-Activity Relationships* (Eds.: S. K. Yang, B. D. Silverman), CRC Press, Boca Raton, FL, **1988**, vol. 2, ch. 2.
- [2] F. A. Beland, R. H. Heflich, P. C. Howard, P. P. Fu in *ACS Symposium Series 283: Polycyclic Hydrocarbons and Carcinogenesis* (Ed.: R. G. Harvey), ACS, Washington, DC, **1985**, ch. 15.
- [3] Y. S. Wu, Y. K. Yang, C. C. Lai, L. E. Unruh, F. E. Beland, P. P. Fu in *Polynuclear Aromatic Hydrocarbons: Measurements, Means, and Metabolism* (11th International Symposium on Polynuclear Aromatic Hydrocarbons) (Eds.: M. Cooke, K. Loening, J. Merritt), Battelle Press, Columbus, OH, **1991**, pp. 1083–1106.
- [4] B. P. Cho, *Org. Prep. Proced. Int.* **1995**, 27, 243–272.
- [5] B. Zielinska, J. Arey, W. P. Harger in “*Polynuclear Aromatic Hydrocarbons: Measurements, Means, and Metabolism* (11th International Symposium on Polynuclear Aromatic Hydrocarbons) (Eds.: M. Cooke, K. Loening, J. Merritt), Battelle Press, Columbus, OH, **1991**, pp. 1107–1126.
- [6] a) J. N. Pitts Jr., B. Zielinska, W. P. Harger, *Mutat. Res.* **1984**, 140, 81–85; b) M. W. Chou, R. H. Heflich, D. A. Casciano, D. W. Miller, J. P. Freeman, F. E. Evans, P. P. Fu, *J. Med. Chem.* **1984**, 27, 1156–1161; c) K. Fukuhara, N. Miyata, M. Matsui, K. Matsui, M. Ishidate Jr., S. Kamiya, *Chem. Pharm. Bull.* **1990**, 38, 3158–3161; d) P. P. Fu, Y.-S. Wu, L. S. Von Tungeln, J.-S. Lai, M. P. Chiarelli, F. E. Evans, *Chem. Res. Toxicol.* **1993**, 6, 603–608; e) G. Dyker, D. Kadzimirsz, A. Thöne, *Eur. J. Org. Chem.* **2003**, 3162–3166.
- [7] a) M. W. Chou, P. P. Fu, *Biochem. Biophys. Res. Commun.* **1983**, 117, 541–548; b) Y.-S. Wu, J.-S. Lai, P. P. Fu, *J. Org. Chem.* **1993**, 58, 7283–7285; c) D. Herreno-Saenz, F. D. Evans, P. P. Fu, *Chem. Res. Toxicol.* **1994**, 7, 806–814.
- [8] P. P. Fu, Y.-C. Ni, Y.-M. Zhang, R. H. Heflich, Y.-K. Wang, J.-S. Lai, *Mutat. Res.* **1989**, 225, 121–125.
- [9] M. J. Lee, J.-S. Lai, P. P. Fu, *Org. Prep. Proced. Int.* **1995**, 27, 595–600.
- [10] a) P. Upadhyaya, L. S. Von Tungeln, P. P. Fu, K. El-Bayoumy, *Chem. Res. Toxicol.* **1994**, 7, 690–695; b) Y.-H. Chae, B.-Y. Ji, J.-M. Lin, P. P. Fu, B. P. Cho, K. El-Bayoumy, *Chem. Res. Toxicol.* **1999**, 12, 180–186; c) Y.-H. Chae, P. Upadhyaya, B.-Y. Ji, P. P. Fu, K. El-Bayoumy, *Mutat. Res.* **1997**, 376, 21–28.
- [11] K. K. Laali in *Carbocation Chemistry* (Eds.: G. A. Olah, G. K. S. Prakash), Wiley, New York, **2004**, ch. 9.
- [12] a) K. K. Laali, T.-M. Liang, P. E. Hansen, *J. Org. Chem.* **1992**, 57, 2658–2667; b) K. K. Laali, S. Bolvig, P. E. Hansen, *J.*

- Chem. Soc. Perkin Trans. 2* **1995**, 537–551; c) K. K. Laali, P. E. Hansen, *J. Chem. Soc. Perkin Trans. 2* **1998**, 1167–1172.
- [13] K. K. Laali, *Coordination Chem. Rev.* **2000**, 210, 47–71.
- [14] a) K. K. Laali, P. E. Hansen, *J. Org. Chem.* **1997**, 62, 5804–5810; b) T. Okazaki, K. K. Laali, B. Zajc, M. K. Lakshman, S. Kumar, W. M. Baird, W.-M. Dashwood, *Org. Biomol. Chem.* **2003**, 1, 1509–1516.
- [15] K. K. Laali, T. Okazaki, *Ann. Rep. NMR Spectrosc.* **2002**, 47, 149–214.
- [16] K. K. Laali, T. Okazaki, P. E. Hansen, *J. Org. Chem.* **2000**, 65, 3816–3828.
- [17] a) A. W. Wood, W. Levin, D. R. Thakker, H. Yagi, R. L. Chang, D. E. Ryan, P. E. Thomas, P. M. Dansette, N. Whittaker, S. Turujman, R. E. Lehr, S. Kumar, D. M. Jerina, A. H. Conney, *J. Biological. Chem.* **1979**, 254, 4408–4415.
- [18] K. Fukuhara, N. Miyata, *Chem. Res. Toxicol.* **1995**, 8, 27–33.
- [19] K. K. Laali, S. Hupertz, A. G. Temu, S. E. Galembach, *Org. Biomol. Chem.* **2005**, 3, 2319–2326.
- [20] A. Musa, B. Sridharan, H. Lee, D. L. Mattern, *J. Org. Chem.* **1996**, 61, 5481–5484 (the reported ^1H NMR data is slightly different!).
- [21] W. Koch, M. C. Holthausen, *A Chemist's Guide to Density Functional Theory*, 2nd ed., Wiley-VCH, Weinheim, **2000**.
- [22] a) A. D. Becke, *Phys. Rev. A* **1988**, 38, 3098–3100; b) C. Lee, W. Yang, R. G. Parr, *Phys. Rev. B* **1988**, 37, 785–789.
- [23] M. J. Frisch, G. W. Trucks, H. B. Schlegel, G. E. Scuseria, M. A. Robb, J. R. Cheeseman, J. A. Montgomery Jr., T. Vreven, K. N. Kudin, J. C. Burant, J. M. Millam, S. S. Iyengar, J. Tomasi, V. Barone, B. Mennucci, M. Cossi, G. Scalmani, N. Rega, G. A. Petersson, H. Nakatsuji, M. Hada, M. Ehara, K. Toyota, R. Fukuda, J. Hasegawa, M. Ishida, T. Nakajima, Y. Honda, O. Kitao, H. Nakai, M. Klene, X. Li, J. E. Knox, H. P. Hratchian, J. B. Cross, C. Adamo, J. Jaramillo, R. Gomperts, R. E. Stratmann, O. Yazyev, A. J. Austin, R. Cammi, C. Pomelli, J. W. Ochterski, P. Y. Ayala, K. Morokuma, G. A. Voth, P. Salvador, J. J. Dannenberg, V. G. Zakrzewski, S. Dapprich, A. D. Daniels, M. C. Strain, O. Farkas, D. K. Malick, A. D. Rabuck, K. Raghavachari, J. B. Foresman, J. V. Ortiz, Q. Cui, A. G. Baboul, S. Clifford, J. Cioslowski, B. B. Stefanov, G. Liu, A. Liashenko, P. Piskorz, I. Komaromi, R. L. Martin, D. J. Fox, T. Keith, M. A. Al-Laham, C. Y. Peng, A. Nanayakkara, M. Challacombe, P. M. W. Gill, B. Johnson, W. Chen, M. W. Wong, C. Gonzalez, J. A. Pople, *Gaussian 03*, Revision B.05, Gaussian, Inc., Pittsburgh, PA, **2003**.
- [24] a) A. E. Reed, F. Weinhold, *J. Chem. Phys.* **1983**, 78, 4066–4073; b) A. E. Reed, R. B. Weinstock, F. Weinhold, *J. Chem. Phys.* **1985**, 83, 735–746.
- [25] K. Wolinski, J. F. Hinton, P. Pulay, *J. Am. Chem. Soc.* **1990**, 112, 8251; R. Ditchfield, *Mol. Phys.* **1974**, 27, 789.

Received: September 3, 2008

Published Online: November 18, 2008